



## PM<sub>10</sub> composition during an intense Saharan dust transport event over Athens (Greece)

E. Remoundaki <sup>a,\*</sup>, A. Bourliva <sup>b,c</sup>, P. Kokkalis <sup>d</sup>, R.E. Mamouri <sup>d</sup>, A. Papayannis <sup>d</sup>, T. Grigoratos <sup>e</sup>, C. Samara <sup>e</sup>, M. Tsezos <sup>a</sup>

<sup>a</sup> National Technical University of Athens (NTUA), School of Mining and Metallurgical Engineering, Laboratory of Environmental Science and Engineering, Heron Polytechniou 9, 15780 Zografou, Greece

<sup>b</sup> Aristotle University of Thessaloniki (AUTH), Department of Geology, 54124 Thessaloniki, Greece

<sup>c</sup> Hellenic Open University, School of Science and Technology, 26335 Patras, Greece

<sup>d</sup> National Technical University of Athens (NTUA), Laser Remote Sensing Laboratory, Heron Polytechniou 9, 15780 Zografou, Greece

<sup>e</sup> Aristotle University of Thessaloniki (AUTH), Department of Chemistry, Environmental Pollution Control Laboratory, 54124 Thessaloniki, Greece

### ARTICLE INFO

#### Article history:

Received 28 March 2011

Received in revised form 8 June 2011

Accepted 8 June 2011

Available online 2 July 2011

#### Keywords:

Saharan dust

Clays

Sulfur

Heavy metals

SEM-EDX

PM<sub>10</sub>

### ABSTRACT

The influence of Saharan dust on the air quality of Southern European big cities became a priority during the last decade. The present study reports results on PM<sub>10</sub> monitored at an urban site at 14 m above ground level during an intense Saharan dust transport event. The elemental composition was determined by Energy Dispersive X-ray Fluorescence Spectrometry (EDXRF) for 12 elements: Si, Al, Fe, K, Ca, Mg, Ti, S, Ni, Cu, Zn and Mn. PM<sub>10</sub> concentrations exceeded the EU limit (50 µg/m<sup>3</sup>) several times during the sampling period. Simultaneous maxima have been observed for the elements of crustal origin. The concentrations of all the elements presented a common maximum, corresponding to the date where the atmosphere was heavily charged with particulate matter permanently for an interval of about 10 h. Sulfur and heavy metal concentrations were also associated to local emissions. Mineral dust represented the largest fraction of PM<sub>10</sub> reaching 79%. Seven days back trajectories have shown that the air masses arriving over Athens, originated from Western Sahara. Scanning Electron Microscopy coupled with Energy Dispersive X-ray analysis (SEM-EDX) revealed that particle agglomerates were abundant, most of them having sizes <2 µm. Aluminosilicates were predominant in dust particles also rich in calcium which was distributed between calcite, dolomite, gypsum and Ca-Si particles. These results were consistent with the origin of the dust particles and the elemental composition results. Sulfur and heavy metals were associated to very fine particles <1 µm.

© 2011 Elsevier B.V. All rights reserved.

### 1. Introduction

The spatial and temporal variability of aerosols and their physico-chemical characteristics such as size and composition affect their roles on climate changes (IPCC, 2007). Mineral dust is a major contributor to aerosol loading, with global flux estimations of 1500–2600 Tg year<sup>-1</sup> (IPCC, 2007). It is estimated that every year, several hundred million tons up to one billion tons of desert dust are exported to the tropical North Atlantic and the Mediterranean Sea (Bonasoni et al., 2004; Prospero 1999; Rodriguez et al. 2001; Sciaré et al. 2003). A number of studies have focused on the long-range transport of Saharan dust over the Mediterranean and their impact to the Mediterranean atmosphere and sea water (Avila et al. 1997;

Bergametti et al. 1989a,b,c; Buat-Menard et al. 1989; Loyer-Pilot et al. 1986; Molinaroli, 1996).

The influence of Saharan dust on the atmospheric particulate matter levels in Southern European countries became a priority during the last decade (Blanco et al. 2003; Gobbi et al. 2007; Moreno et al. 2005; Pappalardo et al., 2010; Papayannis et al., 2005; Papayannis et al., 2008; Rodriguez et al. 2001; Samoli et al. 2011; Querol et al. 2004; Viana et al. 2007). Apart from the fact that the presence of particulate matter in urban environments has several undesirable health effects, a main reason for that special attention was the new limits of the directive for the quality of air in Europe (Directive 2008/50/EC): for PM<sub>10</sub> is determined to be 50 µg/m<sup>3</sup> (limit value already valid since 1/1/2005, not to be exceeded by more than 35 times per calendar year) and for PM<sub>2.5</sub> to be 25 µg/m<sup>3</sup> (target value since 1/1/2010 and limit since 1/1/2015). Mineral dust is a major constituent of PM<sub>10</sub> in southern European big cities. Exceedance cases of the limit of PM<sub>10</sub> due to Saharan dust transport events are often reported. The contribution of Saharan dust in PM<sub>10</sub> concentration levels also complicates the estimation of the impact of the anthropogenic sources to PM<sub>10</sub> and air quality.

\* Corresponding author at: National Technical University of Athens (NTUA), School of Mining and Metallurgical Engineering, Laboratory of Environmental Science and Engineering, Heron Polytechniou 9, 15780 Zografou, Greece. Tel./fax: +30 2107722173.

E-mail address: [remound@metal.ntua.gr](mailto:remound@metal.ntua.gr) (E. Remoundaki).

The atmosphere of the large cities in Greece is very often heavily charged by particulate matter due to both long range transport and local emission sources. The absence of precipitation from spring to late autumn and the favorable conditions for the formation of photochemical smog are also characteristic situations for the big cities in Greece. Monitoring of concentration levels and quantitative estimations on particle composition together with their source identification are necessary in order to acquire data for the estimation of their impact and to answer if the above limits are realistic for the large urban areas in Greece. Results on PM<sub>10</sub> and PM<sub>2.5</sub> concentration levels and composition are recent (appear in literature mainly the last 6 years) for different regions in Greece, pointing out the difficulty to have at present a clear picture of the situation at a national level (Chaloulakou et al. 2003; Lazaridis et al. 2008; Manoli et al. 2002; Terzi et al., 2010; Vassilakos et al. 2005). The results reported from a five-year monitoring of PM<sub>10</sub> at both an urban and a background rural site in Crete (Gerasopoulos et al., 2006), have shown that the EU limit of 50 µg/m<sup>3</sup> was very often exceeded and this was mainly due to dust events for both sites. For the above reasons, every new data set on the variability of concentration levels, the composition and the origins of PM is significant in order to clarify and complete the picture.

The present paper reports the results on PM<sub>10</sub> concentration levels and their composition during an intense Saharan dust transport event over Athens between March 28 and April 3rd, 2009. Experimental results of PM<sub>10</sub> continuous concentration monitoring by TSI DustTrak 8520 and PM<sub>10</sub> sampling on 0.45 µm nucleopore membranes by using TCR TECORA sampler are presented and discussed. The elemental composition, determined by EDXRF using NIST standard SRM 2783 for 12 elements: Si, Al, Fe, K, Ca, Mg, Ti, S, Ni, Cu, Zn, and Mn, is discussed in terms of their temporal variability and the origin of the sampled air masses. Information on air mass origins was acquired by both 7 days back trajectories and wind roses using the data of the local meteorological station. The percentage of the dust contribution and the contribution of both sulfates and mineral dust to the observed PM<sub>10</sub> concentrations was estimated using the experimental data. Scanning Electron Microscopy coupled with Energy Dispersive X ray analysis (SEM-EDX) has been also performed in selected samples. A hundred regions of the selected filters have been analyzed in order to acquire information about the sizes and composition of the PM<sub>10</sub>.

## 2. Materials and methods

### 2.1. PM<sub>10</sub> concentration levels monitoring

PM<sub>10</sub> concentrations were recorded by DustTrak (TSI, Model 8520) (Chan et al., 2002) at the top of the building of the School of Mining and Metallurgical Engineering at the NTUA campus at 14 m above ground level. The sampling point is fully exposed to wind and free all around of other obstacles. DustTrak was selected in order to have a continuous monitoring of PM<sub>10</sub> concentrations during the Saharan dust event and to record their temporal variability with satisfactory time resolution. DustTrak's nominal flow rate is 1.7 l/min and it is obtained by an internal pump integral to the sampler. The monitor is factory calibrated for the respirable fraction of standard ISO12103-1, A1 test dust (Arizona Test Dust), which is representative for a wide variety of aerosols. It measures concentrations in the range of 0.001–100 mg/m<sup>3</sup>, with a resolution of 0.1% of the reading or 0.001 mg/m<sup>3</sup>. Before each measurement, the instrument is zeroed and its flow rate is checked. PM<sub>10</sub> concentrations were recorded from 27/3/2009 until 3/4/2009, every 10 min.

### 2.2. PM<sub>10</sub> sampling and elemental composition determinations-PM<sub>10</sub> SEM-EDX analysis

PM<sub>10</sub> sampling for elemental composition determination and SEM-EDX analysis was carried out using a TCR TECORA (Sentinel PM)

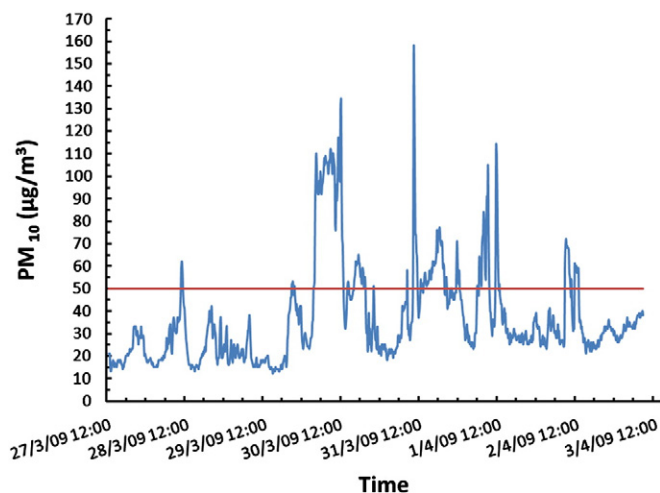


Fig. 1. PM<sub>10</sub> concentrations (in µg/m<sup>3</sup>) between March 27th and April 3rd, 2009.

operating at 38.33 l/min, constructed and calibrated in order to comply with European Standard EN12341 for standard sampling of PM<sub>10</sub>. The sampling device operates with autonomy of 16 samples charged in a charging cassette by programming the sampling span and duration. Aerosol samples were collected on 0.45 µm nucleopore membranes. Twelve samples have been collected between 27/3/2009 and 2/4/2009. From March 28th until April 2nd, two 3-hour samples per day were collected: one beginning in the morning at 9 am local time and the second beginning at 2 pm in order to correspond to urban activities maxima. This 3-hour time span during the two urban activities maxima (beginning and end of working day) was also selected in order to avoid sampling interruption due to filter clogging. Filter clogging is highly probable during periods of highly charged atmosphere by particulate matter as was the case during the dust transport event.

Sampling material and filter keeping petri-dishes were pretreated by soaking in dilute nitric acid solution and thorough rinsing by ultrapure water (18 MΩ/cm) and dried under the laminar flow hood of the laboratory. In order to determine PM<sub>10</sub> concentrations, the nucleopore membranes were weighted before and after sampling according to the procedure described in EN12341 (Annex C) using a Mettler Toledo MS105 with a resolution of 10 µg in the air conditioned weighing room of the laboratory. DustTrak data were used in order to record the concentration variations during the episode of dust transport (Fig. 1, Section 3.1.). The gravimetric data were used for the estimations of the percentage contribution of dust in PM<sub>10</sub> concentrations (Section 3.3.). The regression line for concentrations recorded by DustTrak and those obtained gravimetrically was  $y = 1.23x$  ( $r^2 = 0.89$ ) meaning an overestimation of about 20% for the mean values of the concentrations obtained by DustTrak.

The pre weighted membranes were charged to the filter supports and sampler cassette under the laminar flow hood. Filter blanks and blank field samples were also prepared and analyzed together with

Table 1

Daily mean concentration, minima and maxima observed during the period of interest as recorded by DustTrak TSI 8520.

Date	Mean (µg/m <sup>3</sup> )	Minimum (µg/m <sup>3</sup> )	Maximum (µg/m <sup>3</sup> )
27/03/2009	22	13	33
28/03/2009	25	13	62
29/03/2009	23	12	53
30/03/2009	62	21	134
31/03/2009	46	18	156
01/04/2009	40	23	114
02/04/2009	34	21	72
03/04/2009	33	26	40

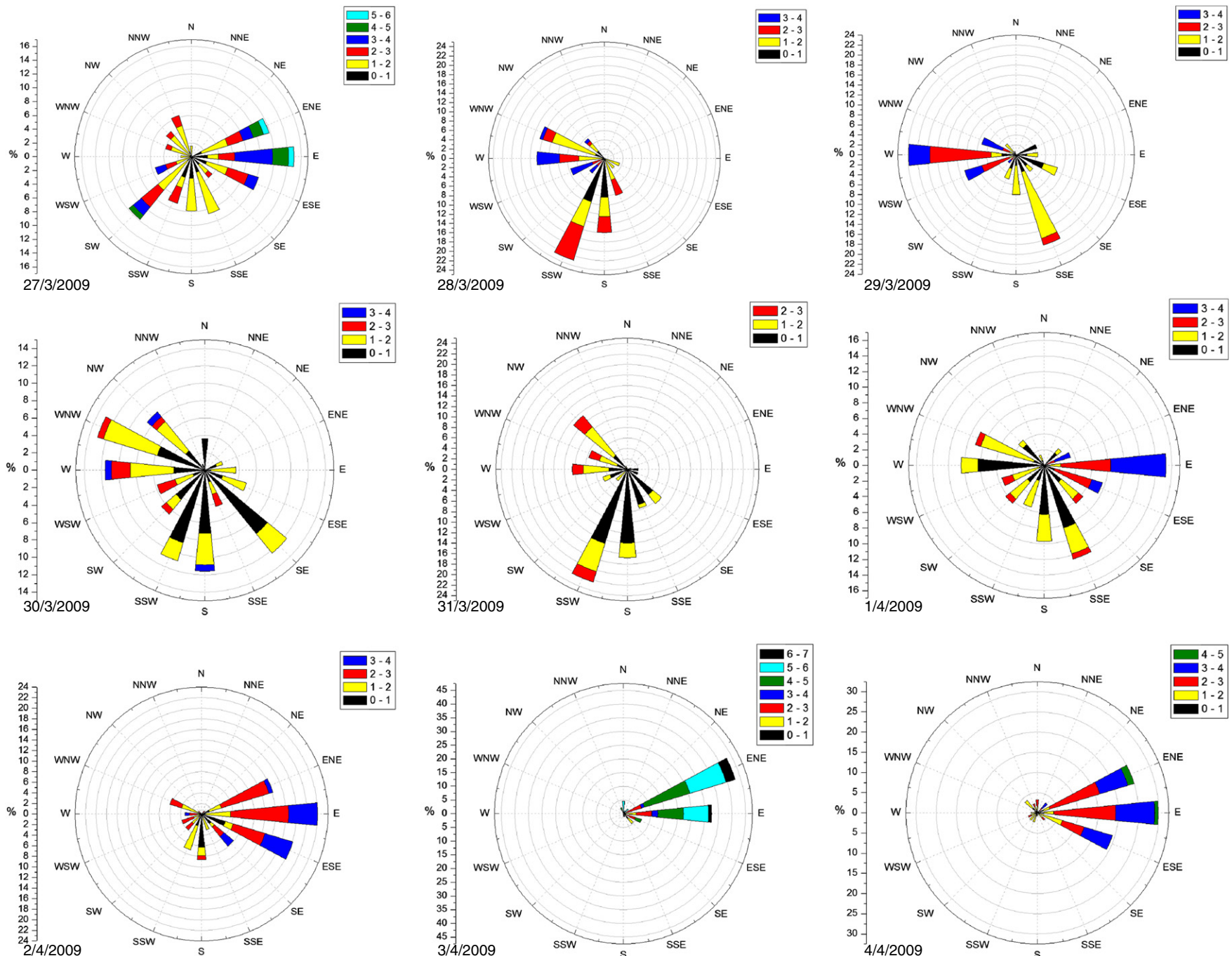


**Fig. 2.** Wind roses as calculated using the data from the local meteorological station of NTUA.

samples. The elemental composition determinations have been carried out by EDXRF (SPECTRO XEPOS bench top XRF spectrometer SPECTRO A.I. GmbH) with Pd end window X-ray tube. NIST standard SRM 2783 has been used for spectrometer calibration verification. The elements Si, Al, Fe, K, Ca, Mg, S, Ni, Cu, Zn, Mn, and Ti, have been determined. A specialized program (SPECTRO X-LAB PRO) was used for values normalization and error correction. The method detection limits were 100 ng/cm<sup>2</sup> for Mg, 20 ng/cm<sup>2</sup> for Al and K, 10 ng/cm<sup>2</sup> for Ca, Ti, Fe, 5 ng/cm<sup>2</sup> for Si, Mn, 2 ng/cm<sup>2</sup> for Ni, 1 ng/cm<sup>2</sup> for S, Cu and Zn. The estimated precision of the method ranged between 0.1% and 30% for individual elements, for most of them being <5% (Terzi et al., 2010).

Three filters have been selected for SEM-EDX analysis. Two filters corresponding to concentrations maxima and major elements maxima observed on 31/3/2009 and a reference-filter sampled before the arrival of the episode of dust transport (27/3/2009) have been analyzed by Scanning Electron Microscope (JEOL JSM-840) – Energy Dispersive X-Ray Spectrometry (Link 10000 AN), operating at an

accelerating potential of 15 kV, probe current <3 nA and analysis time of 60 s. SEM images have been taken and a hundred EDX spectra have been obtained on spots of the three selected samples.

### 2.3. Air mass trajectories and local meteorological data

The HYSPLIT 4 model is a complete system for computing simple trajectories to complex dispersion and deposition simulations using either puff or particle approaches. A discussion of the model is given by Draxler and Hess (1998). In our case, ending air mass backward trajectories were calculated for the Athens site using the Hybrid Single-Particle Lagrangian Integrated Trajectory model (HYSPLIT) to gather information about the origin of the observed aerosols and the synoptic patterns corresponding to the period under study. The calculations were made for the arrival heights of 1, 2 and 3.5 km a.s.l over Athens, Greece (NTUA site).

Wind roses have also been calculated by Microcalc Origin using the local meteorological data from the ground meteorological station of

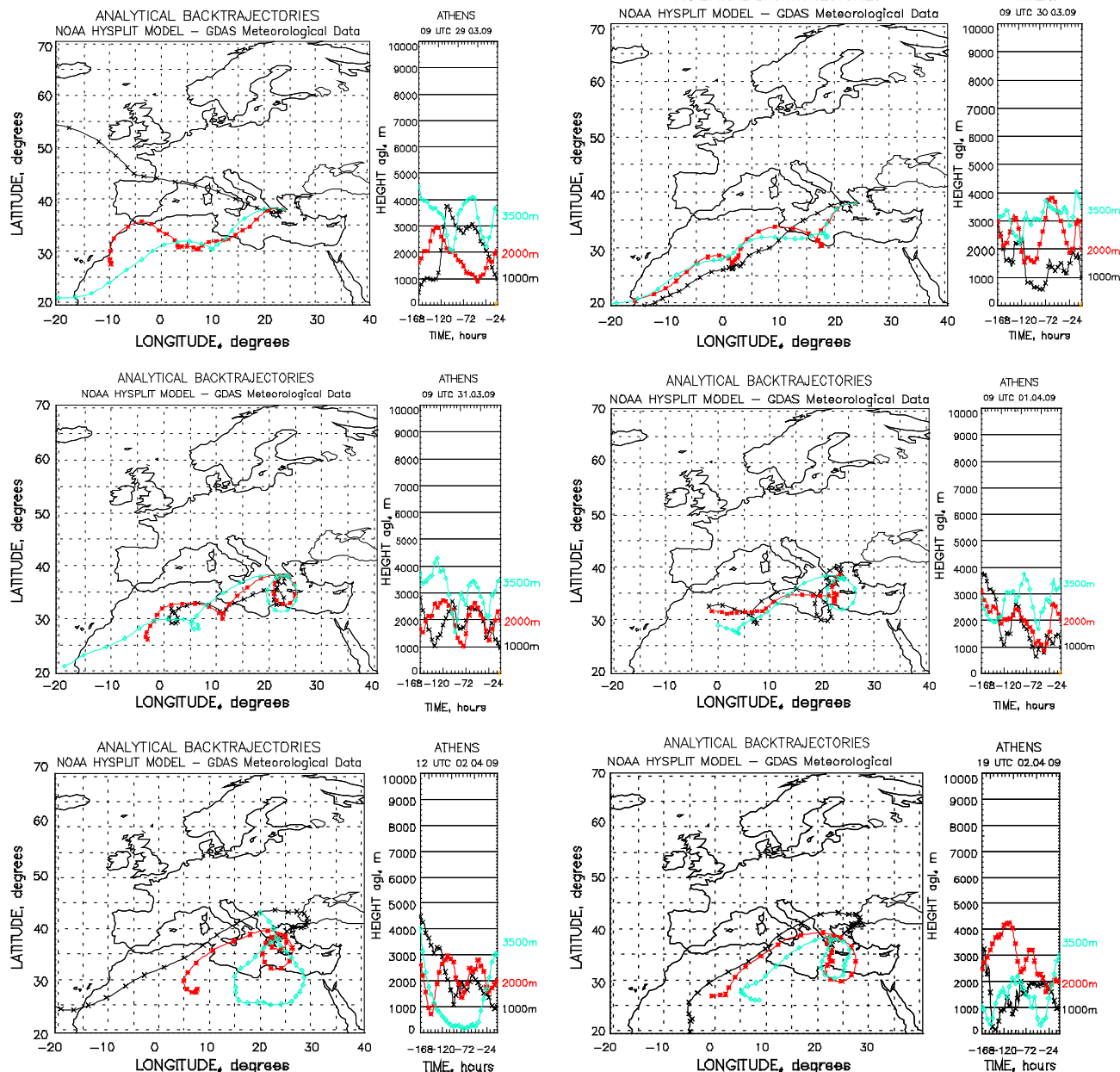


Fig. 3. Seven days air mass back trajectories ending over Athens on March 29th, 30th, 31st April 1st (at 9:00 UTC) and 2nd , 2009 (left: at 12:00 UTC, right: at 19:00 UTC).

NTUA. During the period of interest, no rain has been recorded by the meteorological station of NTUA.

### 3. Results and discussion

#### 3.1. $PM_{10}$ concentration levels

**Fig. 1** presents the recorded  $PM_{10}$  concentrations from March 27th to April 3rd 2009. On the same figure the legislative limit of  $50 \mu\text{g}/\text{m}^3$  is also shown. The recorded concentrations were very often higher than that limit. The minimum value recorded was  $12 \mu\text{g}/\text{m}^3$  on 29/3/2009 and the maximum value  $156 \mu\text{g}/\text{m}^3$  on 31/3/2009. **Table 1**

presents daily mean, min and max values recorded over the period of interest. From this table, it can be seen that mean daily concentrations exceeded the legislation limit of  $50 \mu\text{g}/\text{m}^3$  on March 30 and were very close to that on March 31st and April 1st. **Fig. 2** presents the wind roses obtained from the ground level meteorological station at NTUA for the period under study. From this figure, it is obvious that local winds of south origin were predominant from March 28th until April 1st. From April 2nd, the winds direction changed and east local winds became dominant. It is important to notice that, on March 29th and 30, west winds were also significant.

In **Fig. 3**, the 7 days back-trajectories calculated by the HYSPLIT model for the air masses ending over Athens at 1, 2 and 3.5 km height

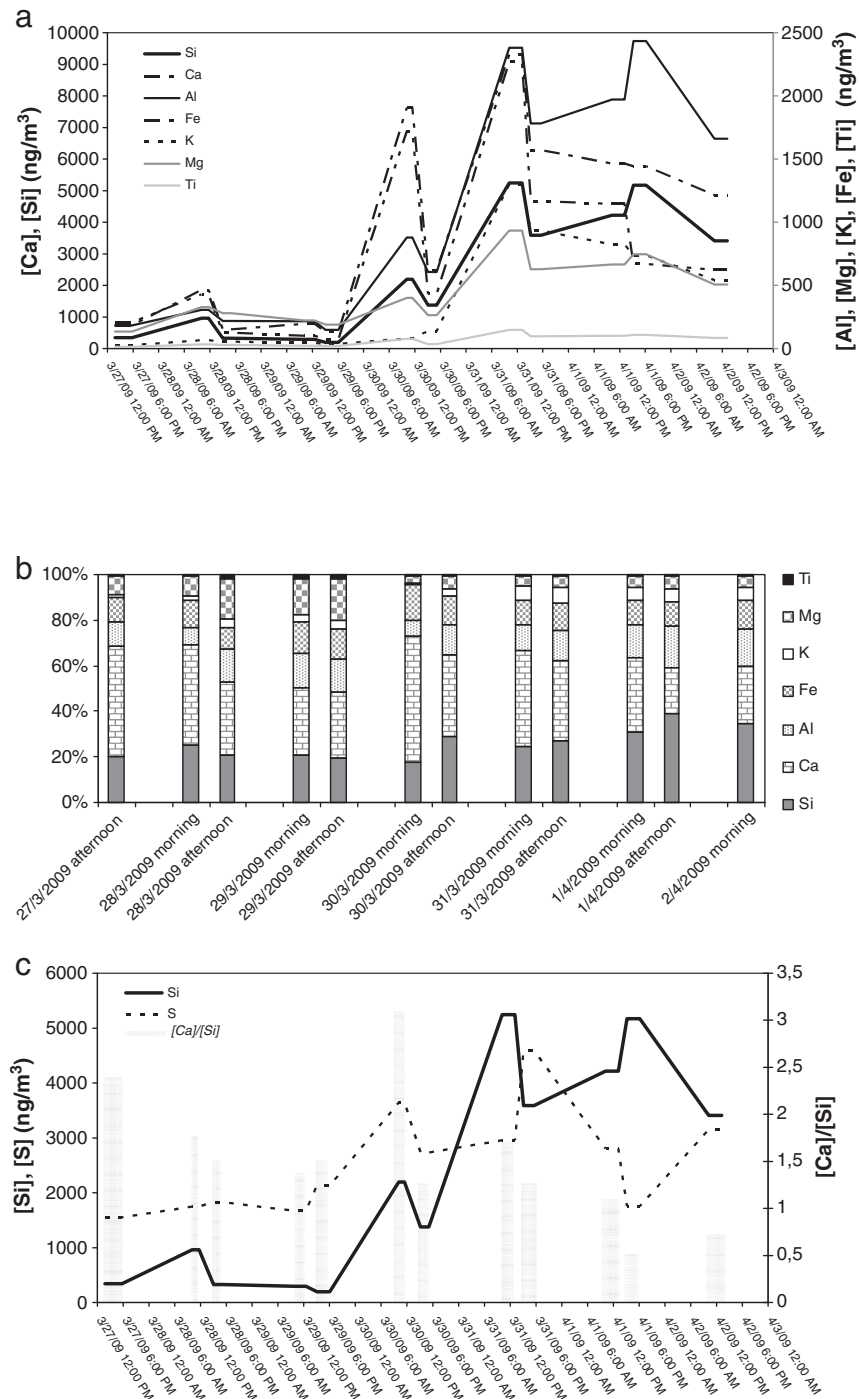


**Fig. 4.** Temporal variability of elemental concentrations of (a) Si, Al, Ca, K, Fe, Mg, Ti (b) percentage distribution of the elements of crustal origin (c) temporal variability of Si and S in  $\text{ng}/\text{m}^3$ , the ratio  $[\text{Ca}]/[\text{Si}]$  is also shown in this figure.

levels are presented. This figure shows that the air masses arriving over Athens on March 29th and 30th originated from Western Sahara and this is clear for the three height levels on March 30th. From March 31st, the origin of the air masses moved towards northern Algeria. From that date, the air masses also were moving anti-cyclonically over Greece, thus also mixing with maritime and local continental aerosols.

From the data presented above, it becomes obvious that the recorded high values of  $\text{PM}_{10}$  concentrations (see Fig. 1) are mainly due to Saharan dust transported over Athens during the period of interest. The magnitude of  $\text{PM}_{10}$  mean daily levels and maxima recorded are in agreement with the findings of earlier studies in the Mediterranean Basin concerning TSP and  $\text{PM}_{10}$  levels during Saharan dust transport events (Gerasopoulos et al., 2006; Gobbi et al. 2007; Kocak et al., 2007; Koulouri et al., 2008; Rodriguez et al. 2001).

### 3.2. Temporal variability of elemental concentrations

Fig. 4a presents the temporal variability of the concentrations of the elements Al, Si, Fe, Ca, K, Mg and Ti. From this figure, it is apparent that the concentrations of these elements present similar temporal variations. The concentrations of the elements of crustal origin presented an abrupt increase on March 30th and were maintained at high levels during the dust transport event from Saharan regions, clearly shown from the backward air mass trajectories (Fig. 3). Concentration levels and concentration maxima of the elements of crustal origin are in agreement to those reported for  $\text{PM}_{10}$  during Saharan dust events. For example, arithmetic mean concentrations for the elements Ca, Fe, Ti in this study are 2986, 973 and 64 ng/m<sup>3</sup> respectively and concentrations maxima 9087, 2328, 147 ng/m<sup>3</sup> respectively. Kocak et al. (2007) reported for dust events arithmetic mean concentration values of Ca, Fe and Ti: 3500, 1200 and 100 ng/m<sup>3</sup> respectively whereas the recorded concentration maxima are even higher than those reported in the present study. Maxima for Ca, Fe and Ti in the coarse fraction reported by Koulouri et al. (2008): 18,615, 8509 and 290 ng/m<sup>3</sup>, although higher, can also be considered in good agreement with those reported in the present study.

The percentage contribution of each element to the total mass of elements of crustal origin is shown on Fig. 4b. Calcium appeared to be the most abundant element among the elements of crustal origin, followed by silicon. Aluminum and iron percentage was of the same order. Potassium and magnesium percentages appeared variable, with a tendency to stabilize to values of about 6% and 5% respectively during the dust episode. Titanium showed an almost stable percentage of about 0.75% (the samples of March 29th showing the most important deviation from this value).

Elemental ratios have been extensively used in order to be compared with those characteristic of different origins. The elemental ratios Al/Si, Ca/Si, Fe/Si, Al/Ca, Ti/Fe and Ti/Ca are reported on Table 2. Al/Si ratio values can be considered as typical for Saharan dust particles (Chiapello et al. 1997; Formenti et al., 2001) as they are close to 0.45. Deviations from that value were observed for the period from

the afternoon of March 28th until the morning of March 30th. The values of Ca/Si ratio exceeded significantly unit except from the last samples where it approached unit and showed values even lower than unit. The observed Ca/Si values can be explained by considering that the long range transported air masses from Saharan sources were mixed with local aerosol sources. Local sources such as road dust and construction works may contribute to the observed elemental concentrations. Ca/Si ratio values in road dust are found to be about 2 and may reach even higher values in urban sites due to construction works (Terzi et al., 2010). On March 29th and 30th, West and WNW winds became important transporting aerosol particles from local urban and industrial regions (Fig. 2). Moreover, Saharan dust originating from Western Sahara is known to be rich in calcite characterized by high Ca/Si ratios: 0.58–0.80 (Avila et al., 1997; Coz et al., 2009; Krueger et al., 2004; Moreno et al., 2005). Dust coming from the Moroccan Atlas region also contains high amounts of dolomite and calcite (Avila et al., 1997). These regions are also origins of Saharan dust transported during the reported period of study which includes air masses originating from more than one Saharan region (Fig. 3). Fe/Si ratio values showed similar behavior to that of Al/Si.

The ratio Al/Ca although variable, showed values similar to those reported in literature for long range transported Saharan dust: 0.33 (Ganor and Foner, 1996), 0.52 and 0.73–0.94 (Borbely-Kiss et al., 2004). The values of the ratios Ti/Fe and Ti/Ca appeared less variable, except for samples corresponding to dates that the influence of local sources was stronger (from the afternoon of March 28th until the morning of March 30th). These ratios also present values similar to those reported in literature for long range transported Saharan dust (Borbely-Kiss et al. 2004; Ganor and Foner 1996).

The above results should be also considered taking into account that Saharan dust is composed of the lighter particles from top soil composition essentially clays and quartz. Clays consist of illite, kaolinite and smectite and, within this group, specifically montmorillonite, in variable proportions (Brooks et al., 2005). Calcite, dolomite and feldspars are also components of transported dust from Northern Africa (Avila et al. 1997; Caquineau et al. 1998; Ganor, 1991; Molinaroli, 1996). Palygorskite is also used as a foot print for Saharan dust emissions from some specific areas (Avila et al. 1997). The relative abundance of one or another type of clay has been linked to the parent material in different regions in North Africa (Molinaroli, 1996; Prospero et al., 2002). Table 3 reports the chemical formula of some representative minerals together with their relative abundance for Western Sahara and Northern Algeria regions. The reported high percentage of Ca in our samples could be attributed in the presence of minerals rich in Ca as for example calcite (Table 3). Iron is present in illite and can also be abundant as hematite (Claquin et al., 1999). According to Fig. 3, such minerals are expected to be present in our samples, where it is clear that the sampled air masses originated from Western Sahara and Northern Algeria.

Fig. 4c presents temporal variations of sulfur concentrations, an element of anthropogenic origin, compared with those of silicon, a

**Table 2**  
Ratios between the elements of crustal origin.

Date	Al/Si	Ca/Si	Fe/Si	Al/Ca	Ti/Fe	Ti/Ca
27/3/2009	0.53	2.39	0.53	0.22	0.07	0.02
28/3/2009	0.32	1.78	0.48	0.18	0.07	0.02
28/3/2009	0.66	1.53	0.46	0.43	0.18	0.06
29/3/2009	0.73	1.38	0.66	0.53	0.11	0.05
29/3/2009	0.76	1.50	0.67	0.50	0.14	0.06
30/3/2009	0.40	3.13	0.87	0.13	0.04	0.01
30/3/2009	0.44	1.25	0.45	0.35	0.06	0.02
31/3/2009	0.45	1.73	0.44	0.26	0.06	0.02
31/3/2009	0.50	1.30	0.44	0.38	0.06	0.02
1/4/2009	0.47	1.09	0.35	0.43	0.07	0.02
1/4/2009	0.47	0.52	0.28	0.91	0.07	0.04
2/4/2009	0.49	0.73	0.36	0.67	0.07	0.03

**Table 3**  
Minerals in Saharan dust and relative abundance according to their origin.

Mineral	Formula	Western Sahara	Northern Algeria
Quartz	$\text{SiO}_2$	+	++
Calcite	$\text{CaCO}_3$	++	++
Kaolinite	$\text{Al}_2\text{Si}_2\text{O}_5(\text{OH})_4$	++	
Illite	$(\text{KH}_3\text{O})(\text{Al},\text{Mg},\text{Fe})_2$	++	++
	$(\text{Si},\text{Al})_4\text{O}_{10}$		
Smectites	Montmorillonite	$(\text{Na},\text{Ca})_{0.33}(\text{Al},\text{Mg})_2$	++
		$(\text{Si}_4\text{O}_{10})(\text{OH})_2 \cdot \text{H}_2\text{O}$	
Palygorskite		$(\text{Mg},\text{Al})_5(\text{Si},\text{Al})_8\text{O}_{20}$	++
		$(\text{OH})_2 \cdot \text{H}_2\text{O}$	

(+ Low, ++ intermediate, +++ high) (Coz et al., 2009).

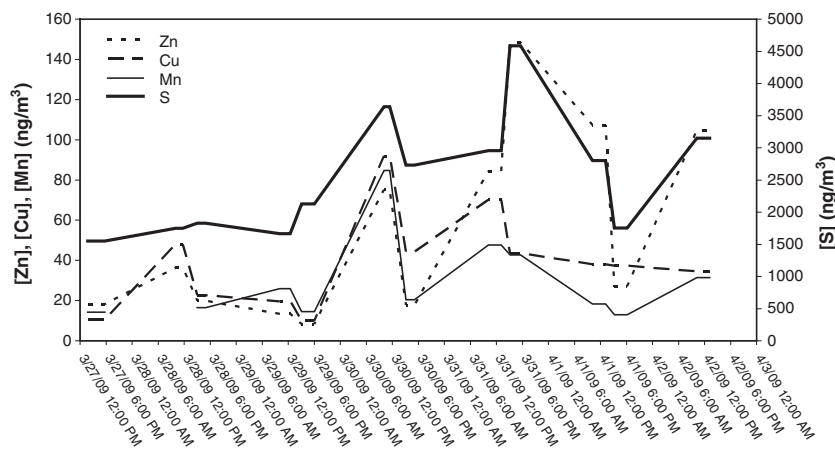


Fig. 5. Temporal variability of elemental concentrations of Zn, Cu and Mn in ng/m<sup>3</sup> compared to that of S.

tracer of crustal origin. On the same figure, the ratio of [Ca]/[Si] is also reported. Sulfur in our samples presents concentration levels usual for urban environments for PM<sub>10</sub> and is mainly present as sulfates (Ho et al., 2006; Sillanpaa et al., 2006; Terzi et al., 2010; Viana et al., 2007; Wang et al., 2005). Sulfates originating from Saharan dust represent a rather small amount, less than 5% (Coz et al., 2009). Until March 30th, sulfur and silicon presented similar temporal variability ending with a maximum for both elements. This behavior can be attributed to the mixing of air masses originating from both long range transport and local emission sources. The wind roses (Fig. 2) corresponding to March 29th and March 30th show the simultaneous presence of south winds, responsible for long range transport of particles of crustal origin and west winds charged with aerosol particles from local urban and industrial emission sources e.g. oil refineries of Aspropyrgos located in the WNW-NW sector (wind rose of March 30th). Moreover, similarities in temporal variations for Si and S, may be also due to formation of coarse sulfate by heterogeneous reactions of gaseous precursors on mineral dust. Hien et al. (2005), pointed out that the yield of nitrate and sulfate formation on mineral dust particles increases with the [Ca]/[Si] ratio. Especially for sulfates, the Ca-richest mineral dust particles correspond to [Ca]/[Si]>1 and are the most

enriched in sulfates (Hien et al. 2005). The yields of such reactions depend on dust mineralogy. For example, Matsuki et al. (2005) found that calcite incorporates the largest amount of sulfur, followed by dolomite, amphibole, clay, feldspar and quartz. In our samples, as already pointed out, the values of this ratio exceed significantly unit until April 1st where are equal to unit and then become lower than unit reaching a value of 0.5. From April 1st, silicon and sulfur concentrations show different temporal variations (Fig. 4c). This is due to the different origin of these elements and probably also to a lower efficiency of mineral dust particles to incorporate sulfur.

The temporal variability of Zn, Cu and Mn concentrations compared to that of sulfur, is shown on Fig. 5. Zinc concentrations present a temporal variability very similar to that of sulfur. Zinc is the most abundant among trace metals in urban environments since it is a marker of wearing particles from tires and brakes. It is also contained in lubricating oil mixed with gasoline for two stroke engines of motorcycles.

Manganese also presents similar variability to that of sulfur but its concentrations may be also influenced by the dust event since Mn is an element of mixed origin: anthropogenic and crustal (Remoudaki et al. 1991). In general the concentrations of Cu, Zn, and Mn are in

**Table 4**  
Percentage of mineral dust (%MIN) and SO<sub>4</sub><sup>2-</sup> contribution to PM<sub>10</sub>.

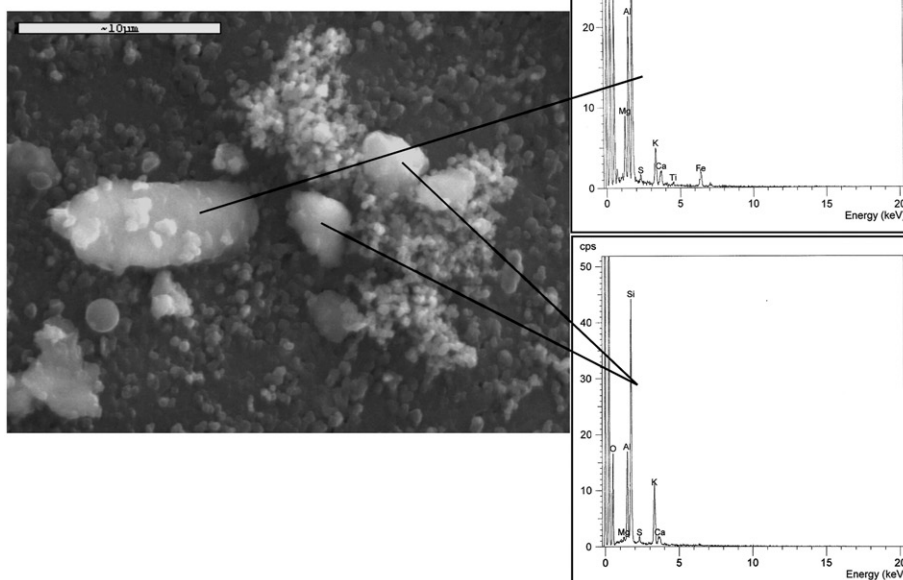
Date	SiO <sub>2</sub> ng/m <sup>3</sup>	Al <sub>2</sub> O <sub>3</sub> ng/m <sup>3</sup>	Fe <sub>2</sub> O <sub>3</sub> ng/m <sup>3</sup>	K <sub>2</sub> O ng/m <sup>3</sup>	CaO + CaCO <sub>3</sub> ng/m <sup>3</sup>	MgO ng/m <sup>3</sup>	TiO <sub>2</sub> ng/m <sup>3</sup>	TOT MIN ng/m <sup>3</sup>	TOT MIN µg/m <sup>3</sup>	PM10 µg/m <sup>3</sup>	%MIN
27/3/2009	736.68	344.70	260.23	32.27	1607.94	222.33	22.36	3226.52	3.2	17	<b>19.0</b>
28/3/2009	2058.96	577.41	661.70	79.22	3334.26	545.76	54.89	7312.19	7.3	39	<b>18.7</b>
28/3/2009	702.82	411.60	217.86	67.41	982.77	464.40	46.71	2893.56	2.9	17	<b>17.0</b>
29/3/2009	631.23	409.23	280.24	53.46	795.33	368.34	37.05	2574.87	2.6	17	<b>15.1</b>
29/3/2009	420.96	280.79	189.35	45.47	575.70	313.25	31.51	1857.02	1.9	14	<b>13.3</b>
30/3/2009	4696.95	1661.57	2727.24	96.67	13397.90	666.03	129.96	23376.32	23.4	68	<b>34.4</b>
31/3/2009	11222.82	4501.17	3328.24	1562.59	17718.74	1550.44	244.56	40128.56	40.1	62	<b>64.7</b>
31/3/2009	7673.18	3368.68	2244.65	1124.99	9090.42	1040.49	162.79	24705.19	24.7	62	<b>39.8</b>
1/4/2009	9021.04	3726.14	2093.12	992.39	8931.27	1101.56	170.38	26035.91	26.0	57	<b>45.7</b>
1/4/2009	11066.15	4600.16	2064.03	886.54	5214.41	1237.48	178.75	25247.53	25.2	32	<b>78.9</b>
2/4/2009	7297.59	3138.37	1733.67	653.30	4854.83	840.20	138.19	18656.15	18.7	54	<b>34.5</b>
Date	S ng/m <sup>3</sup>	SO <sub>4</sub> ng/m <sup>3</sup>	SO <sub>4</sub> µg/m <sup>3</sup>	PM <sub>10</sub> µg/m <sup>3</sup>	%SO <sub>4</sub>	Date	PM <sub>10</sub>	%MIN	%SO <sub>4</sub>	%TOT(MIN + SO <sub>4</sub> )	
27/3/2009	1552.50	4657.51	4.7	17	<b>27.4</b>	27/3/2009	17	19.0	27.4	<b>46.4</b>	
28/3/2009	1748.28	5244.84	5.2	39	<b>13.4</b>	28/3/2009	39	18.7	13.4	<b>32.2</b>	
28/3/2009	1829.40	5488.20	5.5	17	<b>32.3</b>	28/3/2009	17	17.0	32.3	<b>49.3</b>	
29/3/2009	1665.24	4995.71	5.0	17	<b>29.4</b>	29/3/2009	17	15.1	29.4	<b>44.5</b>	
29/3/2009	2127.61	6382.82	6.4	14	<b>45.6</b>	29/3/2009	14	13.3	<b>45.6</b>	<b>58.9</b>	
30/3/2009	3639.75	10919.26	10.9	68	<b>16.1</b>	30/3/2009	68	<b>34.4</b>	16.1	<b>50.4</b>	
31/3/2009	2956.44	8869.33	8.9	62	<b>14.3</b>	31/3/2009	62	<b>64.7</b>	14.3	<b>79.0</b>	
31/3/2009	4586.17	13758.52	13.8	62	<b>22.2</b>	31/3/2009	62	<b>39.8</b>	22.2	<b>62.0</b>	
1/4/2009	2801.99	8405.98	8.4	57	<b>14.7</b>	1/4/2009	57	<b>45.7</b>	14.7	<b>60.4</b>	
1/4/2009	1752.99	5258.98	5.3	30	<b>17.5</b>	1/4/2009	32	<b>78.9</b>	17.5	<b>96.4</b>	
2/4/2009	3148.31	9444.94	9.4	54	<b>17.5</b>	2/4/2009	54	<b>34.5</b>	17.5	<b>52.0</b>	

expected levels for urban environments (Boman et al. 2008; Kwame Aboh et al. 2007; Samara et al. 2003; Terzi et al. 2010; Vanhoof et al. 2003; Voutsas et al. 2002) and probably slightly lower compared to those expected for ground level.

The maximum observed on March 30th for the elements of crustal origin is also observed for trace metals. This maximum corresponds to the interval of the studied period where the PM<sub>10</sub> concentrations were maintained in high levels, >100 µg/m<sup>3</sup>, for about 10 h. The local atmosphere was heavily loaded with long range transported dust

particles which probably were enriched with heavy metals during their transport. PM<sub>10</sub> were further enriched with heavy metals when these air masses mixed with those of local urban and industrial origin. Although the temporal variability of the concentrations of the elements of crustal origin is different from that corresponding to the elements of anthropogenic origin (Fig. 4c), the second maximum observed for the concentrations of elements of anthropogenic origin also corresponds to a period of heavily charged atmosphere with dust particles.

a



b

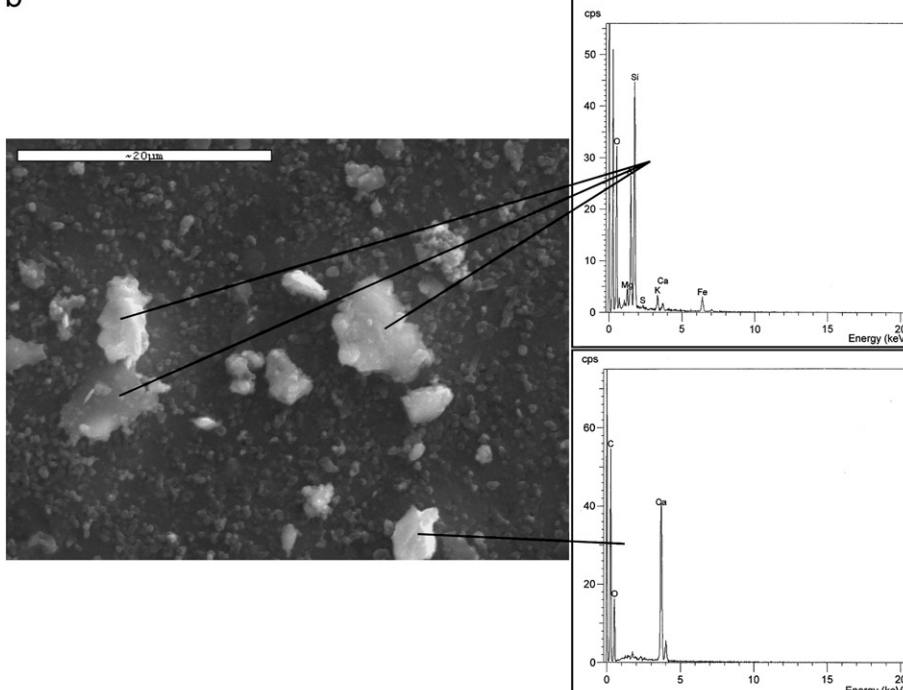


**Fig. 6.** SEM images-EDX spectra (a) illite particles, (b) aluminosilicate particles, probably smectites together with calcite particles, 6(c) aluminosilicate particles, probably smectites.

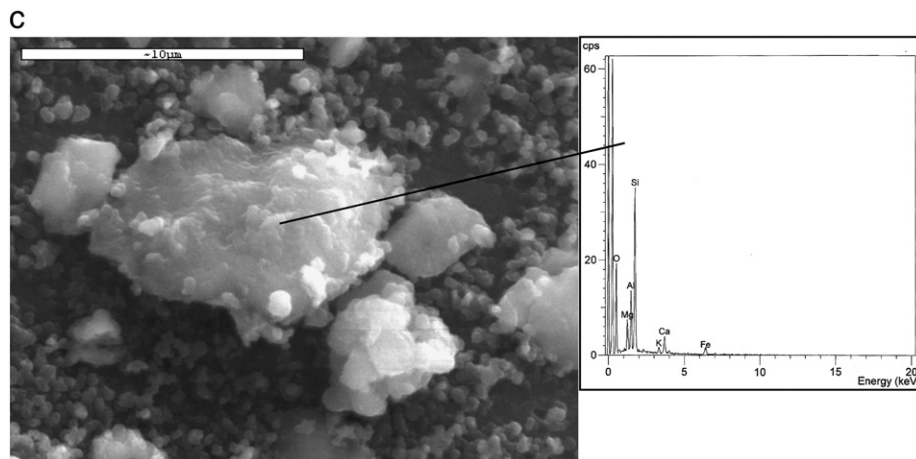


Fig. 6 (continued).

### 3.3. $PM_{10}$ composition-SEM-EDX results

Table 4 presents the concentrations of metals of crustal origin after conversion to their common oxides. Ca was multiplied by a factor of 1.95 to account for  $CaO$  and  $CaCO_3$  which are considered as its most abundant forms (Terzi et al. 2010). These oxides are summed to represent the mineral dust part of  $PM_{10}$ . On the same table, the values of  $PM_{10}$  concentrations, for each filter are reported. From Table 4, it can be seen that the percentage of mineral particles in  $PM_{10}$ , before the arrival of the Saharan dust at the sampling point, ranged from 13 to 19%. From March 30 and during the dust event, the percentage of the mineral particles in  $PM_{10}$  increased significantly reaching 79% on April 1st. These results are in very good agreement with those reported by Gerasopoulos et al. (2006), Kocak et al. (2007) and Koulouri et al. (2008). These authors, also reporting results on dust events monitored in background rural sites, give dust contribution to  $PM_{10}$  levels ranging from 60 to 72% during dust events. It is thus important to mention that during a dust event, dust contribution to  $PM_{10}$  is so important that it could mask any difference between a remote location and a city center.

Assuming that the totality of sulfur was present as sulfates, sulfates were calculated from total sulfur concentrations. Although this may lead to over estimation of the amounts of sulfates, it provides a rather good estimation of their contribution to the  $PM_{10}$  concentrations. The results reported on Table 4, show that the contribution of sulfates to  $PM_{10}$  was significant ranging from about 13% to 30% except from the peak on March 29th where sulfates accounted for about 46% of the total  $PM_{10}$ . The simultaneous presence of west and south winds on this date, explain this high percentage of sulfates and can be clearly seen from the wind rose of 29/3/2009 (Fig. 3). Finally, from Table 4, it can be seen that mineral dust and sulfates may explain about 50% of the total  $PM_{10}$  in absence of Saharan dust transport event. The other main fractions are organic and elemental carbon (about 20–30%, (Sillanpaa et al. 2006)) and particle bound water (20–35% (Tsyro, 2005)). Sea salt particles may account for about 1–5% and trace metals, if calculated as their common oxides, account for less than 1% (Sillanpaa et al. 2006; Terzi et al. 2010). In case of Saharan dust transport event, mineral dust represents the largest fraction of  $PM_{10}$ .

Representative SEM images together with EDX spectra, selected among a significant number of analyzed filter areas (100), are shown following. Fig. 6(a) shows a big diversity of particles of different sizes most of them being submicronic particle agglomerates. The spectra obtained on spots on particles  $>1\text{ }\mu\text{m}$  showed composition characteristic of illite. Fig. 6(b) shows aluminosilicate particles, probably smectites together with calcite particles of about  $1\text{ }\mu\text{m}$ . Fig. 6(c) also shows aluminosilicate particles which are probably smectites.

Fig. 7(a) shows dolomite particles. Fig. 7(b) shows calcium sulfate (gypsum) particles. Iron oxides as those shown in Fig. 7(c) have been often detected in our samples. Fig. 7(d) shows quartz particles. It is important to notice that quartz particles were rare in our samples. Moreover, heavy metals and sulfur were extremely hard or even impossible to be located in most cases showing that these elements were mainly associated to submicronic particles.

Summarizing the above, the SEM images revealed that the filters were rich in particles of submicronic size, very often in agglomerates, together with coarse particles. EDX analysis revealed that aluminosilicates (clays) were predominant. The presence of illite was obvious in many cases, quartz particles were rare and very difficult to be detected. SEM results on dust composition transported over different regions in the Eastern and Western Mediterranean have shown that Al rich clay minerals such as illite and kaolinite are very common in  $PM_{10}$  for Cyprus, are dominant for Crete and in comparable percentage for NE Spain. In all cases Al clays are much more abundant than silica (quartz) (Querol et al., 2009). Dust particles were very rich in calcium which is distributed between calcite, dolomite and sulfates and Ca-Si particles (e.g. smectites). Iron oxides were often detected. These results are in very good agreement and confirm those already reported in the previous paragraphs on the elemental composition of the dust and the origins of the air masses which first became from Western Sahara and moved towards northern Algeria. These findings are also in very good agreement with literature on the Saharan particles characterization and their relationship to their origins (Avila et al., 1997; Caquineau et al., 1998; Coz et al., 2009; Coude-Gaussen et al., 1987; Lange, 1982).

### 4. Conclusions

The high  $PM_{10}$  concentrations recorded at an urban site in Athens for the dates of March 30th, 31st and April 1st 2009 were due to mineral dust particles transported over Athens from Saharan regions. Elements of crustal origin: Al, Si, Fe, Ca, Ti, K, Mg presented high concentrations on the above dates and identical temporal variability over the period of interest.

Seven days back air mass trajectories have shown that the Saharan dust originated from Western Sahara. From March 31st, the origin of the air masses moved towards Northern Algeria. The air masses crossed the central Mediterranean region and moved anti-cyclonically over Greece thus also mixing with local maritime and continental aerosols.

Silicon and calcium were the most abundant among the elements of crustal origin, calcium exhibited higher concentrations than silicon mainly before and in the beginning of the Saharan dust transport event. This result was explained by both considering local sources

such as road dust and construction works and the dust sources. Saharan dust originating from Western Sahara and Northern Algeria is rich in calcium.

Sulfur concentration levels were comparable to those of the elements of crustal origin but showed lower variability than that of the elements of crustal origin due to the dominance of local sources emitting with higher stability than the main sources of the other major elements.

The concentrations of all the elements determined in the present study of both crustal and anthropogenic origin present maxima during the dates where PM<sub>10</sub> concentrations reached elevated values.

A common maximum for all the elements was observed on March 30th where PM<sub>10</sub> concentrations remained higher than 100 µg/m<sup>3</sup> for a period of about 10 h. This can be explained by enrichment of the dust particles with sulfur and trace elements during transport as well as by mixing of the long range transported air masses from Saharan regions with local air masses charged with aerosol particles of urban and industrial origin. The ratio [Ca]/[Si] reached values higher than unit for the period between March 27th and March 31st meaning a strong neutralization capacity for sulfates and thus also contributing to the observed similar temporal variations between sulfur and the elements of crustal origin for this period.

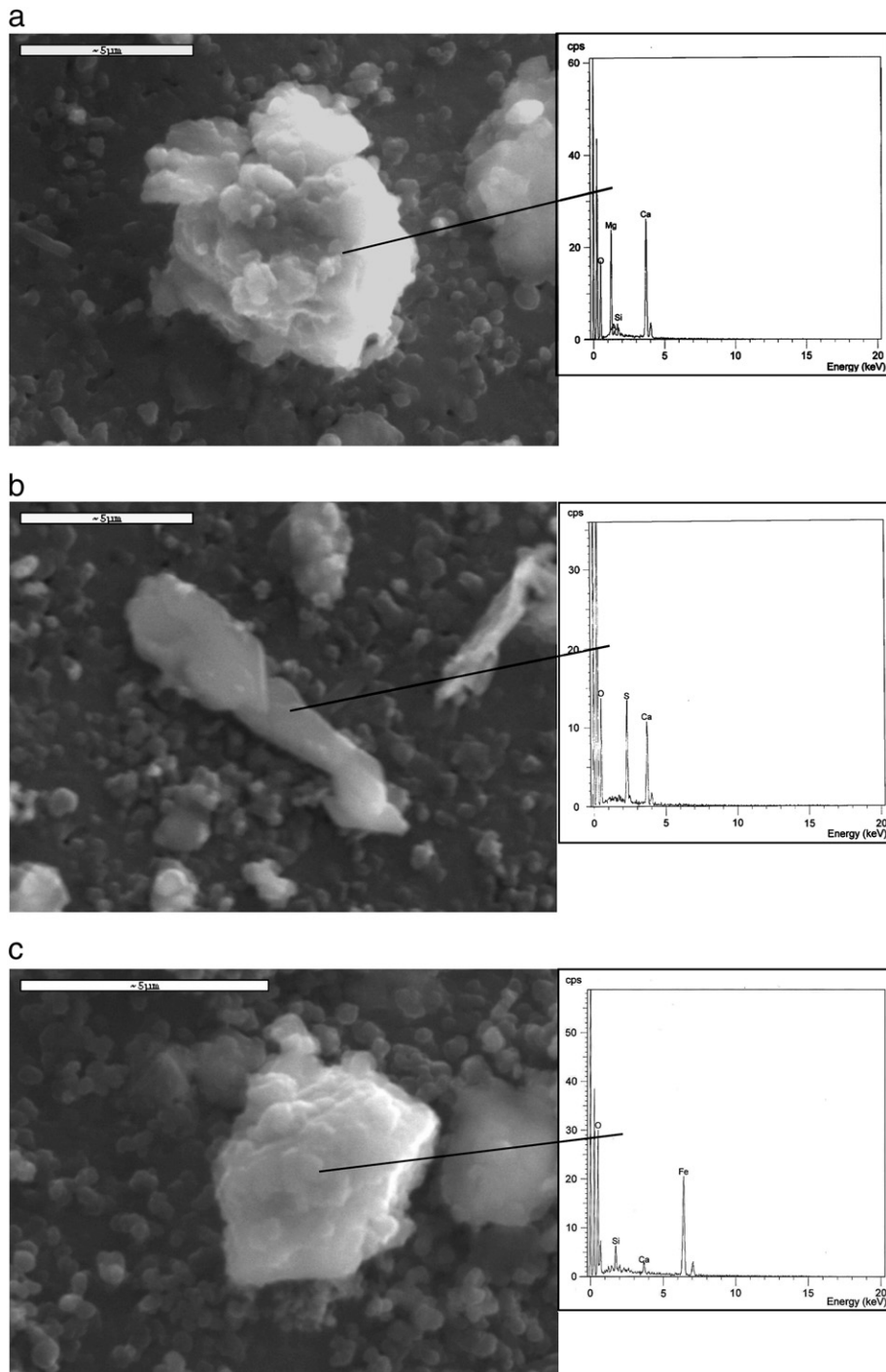


**Fig. 7.** SEM images-EDX spectra (a) dolomite particles, (b) calcium sulfate (gypsum) particles, (c) iron oxides, (d) quartz particles.

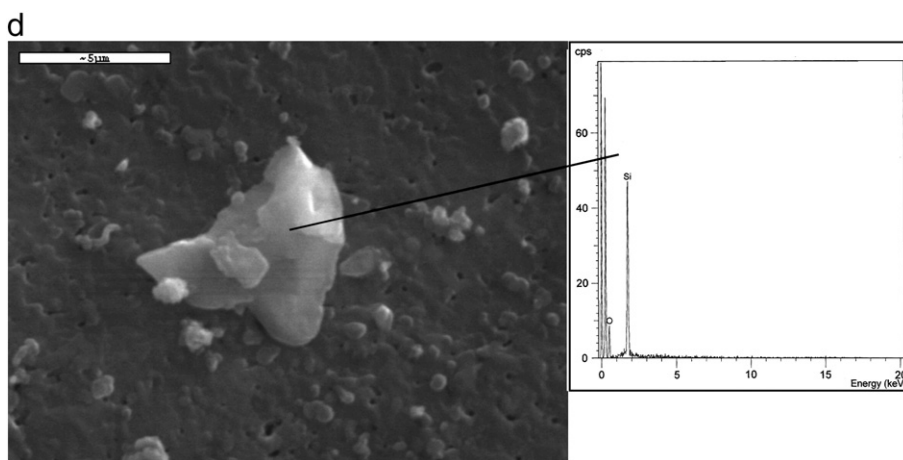


Fig. 7 (continued).

During the dust event, the percentage of the mineral particles in PM<sub>10</sub> increased significantly reaching 79% on April 1st. Sulfates contributed significantly to the total PM<sub>10</sub>.

SEM-EDX results gave important information about the sizes, the morphology and the composition of PM<sub>10</sub>. Most of particles had sizes <2 μm. Dust particles were characterized by a high content in aluminosilicates (clays), while quartz particles were rare. Dust particles were very rich in calcium which is distributed between calcite, dolomite and gypsum and Ca-Si particles. Particles containing iron and iron oxides have been detected by SEM EDX analysis several times. These results confirm the elemental composition results and are consistent with the origin of the dust particles from Western Sahara and Northern Algeria. Heavy metals and sulfur localization was extremely difficult in most cases possibly due to the fact that these elements were associated with ultra-fine particles of sub-micron sizes.

## Acknowledgments

The authors gratefully acknowledge the NOAA Air Resources Laboratory (ARL) for the provision of the HYSPLIT transport and dispersion model and/or READY website (<http://www.arl.noaa.gov/ready.php>) used in this publication.

## References

- Avila A, Queralt-Mitjans I, Alarcon M. Mineralogical composition of African dust delivered by red rains over northeastern Spain. *J Geophys Res* 1997;108:21977–96.
- Bergametti G, Gomez L, Coude-Gaussen G, Rognon P, Le Costumer MN. African dust observed over Canary Island: source regions identification and transport pattern for some summer situations. *J Geophys Res* 1989a;94:14855–64.
- Bergametti G, Gomes L, Remoudaki E, Desbois M, Martin D, Buat-Menard P. Present transport and deposition patterns of African dust to the Northwestern Mediterranean. In: Leinen M, Sarnthein M, editors. Paleoclimatology and Paleometeorology: Modern and Past Patterns of Global Atmospheric Transport, NATO ASI Series No 282. Dordrecht.: Kluwer Publ. Company; 1989b. p. 227–52.
- Bergametti G, Dutot AL, Buat-Menard P, Losno R, Remoudaki E. Seasonal variability of the elemental composition of atmospheric aerosol particles over the Northwestern Mediterranean. *Tellus* 1989c;41:353–61.
- Blanco A, De Tomasi F, Filipo E, Manno D, Perrone MN, Serra A, et al. Characterization of Africal dust over southern Italy. *Atmos Chem Phys* 2003;3:2147–59.
- Boman J, Gatari MJ, Janhall S, Shannigrahi AS, Wagner A. Elemental content of PM2.5 aerosol particles collected in Goteborg during the Gote-2005 campaign in February 2005. *Atmos Chem Phys Discuss* 2008;8:7703–24.
- Bonasoni P, Cristofanelli P, Caltzolari F, Bonafe U, Evangelisti F, Stohl A, et al. Aerosol-ozone correlations during dust transport episodes. *Atmos Chem Phys* 2004;4:1201–15.
- Borbely-Kiss I, Kiss AZ, Koltay E, Szabo Gy, Bozo L. Saharan dust episodes in Hungarian aerosol: elemental signatures and transport trajectories. *J Aerosol Sci* 2004;35:1205–24.
- Brooks N, Chiapello I, Lernia SD, Drake N, Legrand M, Moulin C, et al. The climate-environment society nexus in the Sahara from prehistoric times to the present day. *J North Afr Stud* 2005;10:253–92.
- Buat-Menard P, Davies J, Remoudaki E, Miquel JC, Bergametti G, Lambert C, et al. Non-steady-state biological removal of atmospheric particles from Mediterranean surface waters. *Nature* 1989;340(6229):131–4.
- Caquineau S, Gaudichet A, Gomez L, Magonthier MC, Chatenet B. Saharan dust: clay ratio as a relevant tracer to assess the origin of soil derived aerosols. *Geophys Res Lett* 1998;25:983–6.
- Chaloulakou D, Kassomenos P, Spyrellis N, Demokritou P, Koutrakis P. Measurements of PM10 and PM2.5 particle concentrations in Athens, Greece. *Atmos Environ* 2003;37:649–60.
- Chan LY, Lau WL, Lee SC, Chan CY. Commuter exposure to particulate matter in public transportation modes in Hong Kong. *Atmos Environ* 2002;36:3363–73. 2002.
- Chiapello I, Bergametti G, Catenet B, Bousquet P, Dulac F, Santos Soares E. Origins of African dust transported over the northeastern tropical Atlantic. *J Geophys Res* 1997;102:13701–9.
- Claquin T, Schulz M, Balanski VJ. Modeling the mineralogy of atmospheric dust sources. *J Geophys Res* 1999;104:22243–56.
- Coude-Gaussen G, Rognon P, Bergametti G, Gomez L, Strauss B, Gros JM, et al. Saharan dust over Fuerteventura island (Canaries): chemical and mineralogical characteristics, airmass trajectories, and probable sources. *J Geophys Res* 1987;92:9753–71.
- Coz E, Gomez-Moreno FJ, Pujadas M, Casuccio GS, Lersh TL, Artinao B. Individual particle characteristics of North Africian dust under different long-transport scenarios. *Atmos Environ* 2009;43:1850–63.
- Directive 2008/50/EC of the European Parliament and of the Council of 21 May 2008 on ambient air quality and cleaner air for Europe.
- Draxler RR, Hess GD. An overview of the hysplit\_4 modeling system for trajectories, dispersion, and deposition. *Australian Meteorological Magazine* 1998;47:295–308.
- Formenti P, Andreae MO, Lange L, Roberts G, Cafmeyer J, Rajta I, et al. Saharan dust in Brasil and Suriname during the Large scale Biosphere–Atmosphere Experiment in Amazonia (LBA)-Cooperative LBA Regional Experiment (CLAIRE) in March 1998. *J Geophys Res* 2001;106(D14):14919–34.
- Ganor E. The composition of clay minerals transported to Israel as indicators of Saharan dust emission. *Atmos Environ* 1991;25A:2657–64.
- Ganor E, Foner HA. The mineralogical and chemical properties and the behaviour of Aeolian Saharan dust over Israel. In: Gurezon S, Chester R, editors. The impact of desert dust across the Mediterranean. Dordrecht: Kluwer Academic Publishers; 1996. p. 163–72.
- Gerasopoulos E, Kouvarakis G, Babasaki P, Vrekoussis M, Putaud J-P, Mihalopoulos N. Origin and variability of particulate matter (PM10) mass concentrations over the Eastern Mediterranean. *Atmos Environ* 2006;40:4679–90.
- Gobbi GP, Barnaba F, Ammannato L. Estimating the impact of Saharan dust on the year 2001 PM10 record of Rome, Italy. *Atmos Environ* 2007;41:261–75.
- Hien PD, Bae VD, Thinh NTH. Investigation of sulphate and nitrate formation on mineral dust particles by receptor modelling. *Atmos Environ* 2005;39:7231–9.
- Ho KF, Lee SC, Cao JJ, Chow JC, Watson JG, Chan CK. Seasonal variations and mass closure analysis of particulate matter in Hong Kong. *Sci Total Environ* 2006;355:276–87.
- IPCC Climate change. Synthesis report. Contribution of working Groups I, II and III to the Fourth Assessment Report of intergovernmental Panel on climate change. In: Pachauri RK, Reisinger A, editors. Core Writing Team. Geneva, Switzerland: IPCC; 2007. p. 104.
- Kocak M, Mihalopoulos N, Kubilay N. Chemical composition of the fine and coarse fraction of aerosols in the northeastern Mediterranean. *Atmos Environ* 2007;41:7351–68.
- Koulouri E, Saarikoski S, Theodosi C, Markaki Z, Gerasopoulos E, Kouvarakis G, et al. Chemical composition and sources of fine and coarse aerosol particles in the Eastern Mediterranean. *Atmos Environ* 2008;42:6542–50.
- Krueger BJ, Grassian VH, Cowin JP, Laskin A. Heterogeneous chemistry of individual mineral dust particles from different source regions: the importance of particle mineralogy. *Atmos Environ* 2004;38:6253–61.
- Kwame Aboh IJ, Henriksson D, Laursen J, Lundin M, Pind N, Lindgren ES, et al. EDXRF characterization of elemental contents in PM2.5 in a medium sized Swedish city dominated by a modern incineration plant. *X-Ray Spectrom* 2007;36:104–10.

- Lange H. Distribution of chlorite and kaolinite in eastern Atlantic sediments off North Africa. *Sedimentology* 1982;29(3):427–31.
- Lazaridis M, Dzumbova L, Kapanakis I, Ondracek J, Glytsos T, Aleksandropoulou V, et al. PM10 and PM2.5 levels in the Eastern Mediterranean (Akrotiri Research Station, Crete, Greece). *Water Air Soil Pollut* 2008;189:85–101.
- Loye-Pilot MD, Martin JM, Morelli J. Influence of Sahara dust on the rain acidity and atmospheric input to the Mediterranean. *Nature* 1986;321:427–8.
- Manoli E, Voutsas D, Samara C. Chemical characterization and source identification/appportionment of fine and coarse air particles in Thessaloniki, Greece. *Atmos Environ* 2002;36:949–61.
- Matsuki A, Iwasaka Y, Shi G, Zhang D, Trochkin D, Yamada M, Kim Y-S, Chen B, Nagatani T, Miyazawa T, Nagatani M, Nakata H. Morphological and chemical modification of mineral dust: observational insight into the heterogeneous uptake of acidic gases. *Geophys Res Lett* 2005;32:L22806. doi:10.1029/2005GL024176.
- Molinaroli E. Mineralogical characterization of Saharan dust with a view to its final destination in Mediterranean sediments. In: Guerzoni S, Chester R, editors. The impact of Desert dust Across the Mediterranean. The Netherlands: Kluwer Academic Publishers; 1996. p. 153–62.
- Moreno T, Querol X, Alastuey A, Viana M, Gibbons W. Exotic dust intrusions into the central Spain: implications for legislative controls on atmospheric particles. *Atmos Environ* 2005;39:6109–20.
- Papayannis A, Balis D, Amiridis V, Chourdakis G, Tsaknakis G, Zerefos C, et al. Measurements of Saharan dust aerosols over the Eastern Mediterranean using elastic backscatter-Raman lidar, spectrophotometric and satellite observations in the frame of the EARLINET project. *Atmos Chem Phys* 2005;5:2065–79.
- Papayannis A, Amiridis V, Mona L, Tsaknakis G, Balis D, Bosenberg J, et al. Pietruczuk, Pisani, G., Ravetta, F., Rizi, V., Sicard, M., Trickl, T., Wiegner, M., Gerding, M., Mamouri, R.E., D'Amico, G., Pappalardo, G., Systematic lidar observations of Saharan dust over Europe in the frame of EARLINET (2000–2002). *J Geophys Res* 2008;113:D10204. doi:10.1029/2007JD009028.
- Pappalardo G, Wandinger U, Mona L, Hiebsch A, Mattis I, Amodeo A, et al. EARLINET correlative measurements for CALIPSO: first intercomparison results. *J Geophys Res* 2010;115:D00H19. doi:10.1029/2009JD012147.
- Prospero JM. Long-term measurements of the transport of African Mineral dust to the southeastern United States: implications for regional air quality. *J Geophys Res* 1999;104:15917–27.
- Prospero JM, Ginoux P, Torres JO, Nicholson SE. Environmental characterization of global sources of atmospheric soil dust identified with the nimbus 7 total ozone mapping spectrometer (TOMS) absorbing aerosol product. *Rev Geophys* 2002;40:2–32.
- Querol X, Alastuey A, Rodriguez S, m Viana MM, Artinano B, Salvador P, et al. Levels of particulate matter in rural urban and industrial sites in Spain. *Sci Total Environ* 2004;359:76.
- Querol X, Pey J, Pandolfi M, Alastuey A, Cusack M, Perez N, et al. African dust contributions to mean ambient PM10 mass-levels across the Mediterranean Basin. *Atmos Environ* 2009;43:4266–77.
- Remoundaki E, Bergametti G, Losno R. On the dynamic of the atmospheric input of copper and manganese into the Western Mediterranean Sea. *Atmos Environ* 1991;25A(3/4):733–44.
- Rodriguez S, Querol X, Alastuey A, Kallos G, Kakaliagou O. Saharan dust contribution to PM10 and TSP levels in southeastern and eastern Spain. *Atmos Environ* 2001;35:2433–47.
- Samara C, Koumtzis T, Tsitouridou R, Kanas G, Simeonov V. Chemical mass balance source apportionment of PM10 in an industrialized urban area of Northern Greece. *Atmos Environ* 2003;37:41–54.
- Samoli E, Kougea E, Kassomenos P, Analitis A, Katsouyanni K. Does the presence of desert dust modify the effect of PM<sub>10</sub> on mortality in Athens, Greece? *Sci Total Environ* 2011;409(11):2049–54.
- Sciare J, Bardouki H, Moulin C, Mihalopoulos N. Aerosol sources and their chemical contribution to the chemical composition of aerosols in the Eastern Mediterranean Sea during summertime. *Atmos Chem Phys* 2003;3:291–302.
- Sillanpaa M, Hillamo R, Saarikoski S, Frey A, Pennanen A, Makkonen U, et al. Chemical composition and mass closure of particulate matter at six urban sites in Europe. *Atmos Environ* 2006;40:5212–23.
- Terzi E, Argyropoulos G, Bougatioti A, Mihalopoulos N, Nikolaou K, Samara C. Chemical composition and mass closure of ambient PM10 at urban sites. *Atmos Environ* 2010;44:2231–9.
- Tsyro SG. To what extend can aerosol water explain the discrepancy between model calculated and gravimetric PM10 and PM2.5. *Atmos Chem Phys* 2005;5:515–32.
- Vanhoof C, Chen H, Berghmans P, Corthouts V, De Brucker N, Tirez, KA risk assessment study of heavy metals in ambient air by WD XRF spectrometry using aerosol-generated filter standards. *X-Ray Spectrom* 2003;32:129–38.
- Vassilakos C, Saraga D, Maggos T, Michopoulos J, Pateraki C, Helmis CG. Temporal variations of PM2.5 in the ambient air of a suburban site in Athens, Greece. *Sci Total Environ* 2005;349:223–31.
- Viana M, Maenhaut W, Chi X, Querol X, Alastuey A. Comparative chemical mass closure of fine and coarse aerosols at two sites in south and west Europe: implications for EU air pollution policies. *Atmos Environ* 2007;39:5865–75.
- Voutsas D, Samara C, Koumtzis Th, Ochsenkuhn K. Elemental composition of airborne particulate matter in the multi-impacted urban area of Thessaloniki, Greece. *Atmos Environ* 2002;36:4453–62.
- Wang H, Kawamura K, Shooter D. Carbonaceous and ionic components in wintertime aerosols from two New Zealand cities: implications for solid fuel combustion. *Atmos Environ* 2005;39:5865–75.